Published in final edited form as:
Proteomics. 2008 August ; 8(16): 3210–3220. doi:10.1002/pmic.200800157.

Focused glycomic analysis of the *N*-linked glycan biosynthetic pathway in ovarian cancer

Karen L. Abbott[1], **Alison V. Nairn**[1], **Erica M. Hall**[1], **Marc B. Horton**[2], **John F. McDonald**[3,4], **Kelley W. Moremen**[1], **Daniela M. Dinulescu**[2], and **Michael Pierce**[1]

[1]Complex Carbohydrate Research Center and Department of Biochemistry and Molecular Biology and Department of Chemistry, University of Georgia, Athens, GA, USA

[2]Department of Pathology, Brigham and Women's Hospital, Harvard Medical School, Boston, MA, USA

[3]School of Biology, Georgia Institute of Technology, Atlanta, GA, USA

[4]Ovarian Cancer Institute, Atlanta, GA, USA

Abstract

Epithelial ovarian cancer is the deadliest female reproductive tract malignancy in Western countries. Less than 25% of cases are diagnosed when the cancer is confined, however, pointing to the critical need for early diagnostics for ovarian cancer. Identifying the changes that occur in the glycome of ovarian cancer cells may provide an avenue to develop a new generation of potential biomarkers for early detection of this disease. We performed a glycotranscriptomic analysis of endometrioid ovarian carcinoma using human tissue, as well as a newly developed mouse model that mimics this disease. Our results show that the *N*-linked glycans expressed in both non-diseased mouse and human ovarian tissues are similar; moreover, malignant changes in the expression of *N*-linked glycans in both mouse and human endometrioid ovarian carcinoma are qualitatively similar. Lectin reactivity was used as a means for rapid validation of glycan structural changes in the carcinomas that were predicted by the glycotranscriptome analysis. Among several changes in glycan expression noted, the increase of bisected *N*-linked glycans and the transcripts of the enzyme responsible for its biosynthesis, GnT-III, was the most significant. This study provides evidence that glycotranscriptome analysis can be an important tool in identifying potential cancer biomarkers.

Keywords

Bisecting; Cancer; Glycan; Glycoprotein; Tissue

1 Introduction

The glycosylation patterns of cell surface glycoproteins play important roles in mediating cell–cell and cell–matrix interactions. During oncogenesis, distinct signal transduction pathways are altered, leading to the differential expression of numerous genes. Genes known as glycosyltransferases (GT) and glycosylhydrolases (GH), responsible for the addition and

Correspondence: Dr. Karen Abbott, Complex Carbohydrate Research Center, University of Georgia, Athens, GA 30602, USA, kabbott@uga.edu, **Fax:** 11-706-542-4412.

The authors have declared no conflict of interest.

removal of sugars on proteins in the ER and Golgi apparatus, can change activity during oncogenesis, causing different oligosaccharide structures to emerge on cell surface glycoproteins [1, 2]. These glycan changes can have potent effects on the tumor microenvironment, promoting tumor invasion and metastasis [3–6]. Factors contributing to the regulation of glycosylation include: nucleotide sugar donor availability, substrate availability, sequential reactions, and transcriptional regulation of GT and GH. Studies examining the dynamics of the glycome during differentiation of stem cells have found that changes in GT and GH mRNA levels correlate well with glycan structures observed [7]. Therefore, despite the complexity of factors influencing glycosylation, transcriptional regulation of the enzymes involved in the synthesis and catabolism of glycans seems to be the one of the primary mechanisms to control glycan structures on the cell surface. Comparative studies examining the differences in GT and GH expression patterns between normal and tumor tissue could direct the discovery of tumor-specific glycosylation changes associated with particular malignancies, which could then be exploited to develop diagnostic and cell targeting reagents.

Epithelial ovarian cancer is the deadliest reproductive tract malignancy of women in Western countries [8]. Ovarian cancer survival rates at 5 years are only 30% for women diagnosed with distant metastases; however, the percentage survival climbs to 90% for women diagnosed with disease confined to the ovary [9]. Unfortunately, fewer than 25% of women are diagnosed when the disease is confined, due primarily to the lack of screening tests capable of detecting ovarian cancers early. Epithelial ovarian cancers are comprised of five major subtypes (serous, endometrioid, mucinous, clear cell, and transitional adenocarcinomas), with serous and endometrioid being the two most common types. Several oncogenes have been implicated in ovarian cancer development including: *c-myc, k-ras, erbB2, egfr, p53,* β*-catenin, brca1/2, pten,* and others [10–12].

The use of mouse models that recapitulate human ovarian cancer can significantly elevate our understanding of the molecular pathogenesis of this malignancy. Epithelial ovarian cancer arises in humans from the ovarian surface epithelium (OSE), epithelial inclusion cysts, or the tubal fimbria [13, 14]. Utilizing this knowledge, a mouse model of human epithelial endometrioid ovarian carcinoma was developed by adenoviral infection of the Cre recombinase in the OSE of conditional mice engineered to activate oncogenic *k-ras* and inactivate *pten* [12]. The combination of these mutations leads to the induction of malignant epithelial endometrioid ovarian carcinoma lesions that recapitulate the morphology and histology of the human disease [12]. Most recently, several clinical studies have validated these genetic results by identifying the first cases of human ovarian carcinomas with synchronous *k-ras* and *pten* mutations [15, 16]. These data indicating genetic similarity between mouse and human ovarian carcinoma prompts us to ask if glycosylation changes occurring as a consequence of synchronous *k-ras* and *pten* mutations are similar in both mouse and human ovarian carcinoma. We have used a quantitative real-time PCR approach (qRT-PCR) to quantitatively measure changes in the expression levels of enzymes in the *N*-linked biosynthetic pathway for mouse and human epithelial ovarian endometrioid carcinomas. Comparative lectin blot analysis was used to confirm changes in glycan structures predicted by qRT-PCR results.

2 Materials and methods

2.1 Tumor samples

Endometrioid ovarian tumors ($N = 3$) and normal ovaries ($N = 6$) were obtained from the previously described mouse model [12]. Tumors were graded and assessed based on established histopathology analysis [12]. Human endometrioid ovarian cancers ($N = 3$) (>90% tumor) were obtained from women as frozen tissue from the Ovarian Cancer Institute

(Atlanta, GA). Institutional Review Board approval was obtained for this research. Human normal adjacent ovary RNA samples ($N = 2$) were purchased from BioChain Institute (Heyward, CA). Human normal ovary tissue lysate was purchased from Protein Biotechnologies (Ramona, CA).

2.2 qRT-PCR

Samples (50 mg tissue for tumor, entire normal ovaries) were extracted using 0.8 mL TriZol (Invitrogen, Carlsbad, CA) with polytron homogenization at setting 3 for 1 min. Total RNA was isolated according to the manufacturer's instructions. After DNase treatment, RNA (2 μg) was reverse transcribed using Superscript III (Invitrogen) with random hexamers and Oligo (dT). Primer pairs for assay genes and control genes were designed within a single exon using conditions described in Nairn *et al*. [38] and listed in Supporting Information Table 1. Primers were validated with respect to primer efficiency and single product detection. The control gene, Ribosomal Protein L4 (RPL4, NM_024212) was included on each plate to control for run variation and to normalize individual gene expression. Samples were run with negative control templates prepared without reverse transcription to ensure amplification is specific to cDNA. Triplicate Ct values for each gene were averaged and the SD from the mean was calculated. Data were converted to linear values and normalized as described previously [7].

2.3 Lectin analysis

Tissue (50 mg) isolated from the same tumors used for qRT-PCR analysis were lysed in RIPA buffer (1 × PBS, 1% NP-40, 0.5% DOC, 0.1% SDS) containing a mini complete protease inhibitor tablet (Roche, Indianapolis, IN) using a polytron at setting 3 for 1 min. The lysate was cleared by centrifugation at 10 000 × *g* for 10 min. Protein concentrations were determined by BCA assay (Pierce, Rockford, IL). Biotinylated lectin (Con A, Vector Labs, Burlingame, CA) (2 μg) was added to 50 μg cleared lysate at 4°C for 2 h. Paramagnetic streptavidin beads (50 μL) were added to separate Con A bound and unbound proteins. Unbound fractions, 10 μg, were separated on 4–12 % NuPage Bis Tris gels and transferred to PVDF membrane at 25 V for 1.5 h. Membranes were blocked overnight in 3% BSA/TBST buffer before lectin blot detection using a 1:5000 dilution of the following biotinylated lectins: (*Phaseolus vulgaris leucoagglutinin* (L-PHA), *P. vulgaris erythroagglutinin* (E-PHA), *Aleuria aurantia* (AAL), and *Datura stramonium* (DSL), Vector Labs). Bound lectin was detected using a 1:5000 dilution of streptavidin–HRP (Vector Labs) before washing and detection using Western Lightening Plus (Perkin Elmer).

3 Results

3.1 Expression data from the *N*-linked biosynthetic pathway for normal ovary

Enzymes from the *N*-linked glycosylation pathway (Fig. 1A) were chosen for analysis based on low levels of redundancy and the previous correlations of transcript levels with glycan structural analysis in mouse tissues [38]. Before analyzing tumor tissues, we examined the relative transcript abundance of these enzymes using pooled RNA isolated from normal mouse and human ovarian tissue. The development of epithelial endometrioid ovarian tumors in the model developed by Dinulescu *et al*. [12] utilizes adenoviral infection of the Cre recombinase into the outer epithelial layer of the ovary to initiate tumor formation. This technique allows the noninfected ovary within the same animal to serve as a normal control. From the group of genes analyzed, there are both similarities and differences in transcript expression profiles between mouse and human normal ovary. Transcripts present in higher abundance for both species are: FUT8, MGAT1 (human) or MGAT2 (mouse), and MGAT5 (Figs. 1B and C). These enzymes are involved in the branching (MGAT1, MGAT2, MGAT5) or core fucosylation (FUT8) of *N*-linked glycans (Fig. 1A). Due to the higher

levels of these transcripts, core fucosylated hybrid type or core fucosylated complex branched *N*-linked glycans are likely to be abundant in both mouse and human ovary. The MGAT3 transcripts are present at low levels in both mouse and human ovaries (Figs. 1B and C). The lower levels of MGAT3 transcripts suggest that bisecting *N*-linked glycans may be present at a lower levels in normal mouse and human ovary tissue. Interestingly, the levels of MGAT4b transcripts are very high in mouse compared with human. However, for both mouse and human the MGAT4a levels are lower. These genes are both capable of adding *N*-acetylglucosamine in β(1,4) linkage (Fig. 1A). Considering the levels of both MGAT4a and MGAT4b, along with abundant MGAT5 levels, tri- and tetra-antennary complex *N*-linked glycans should be present in normal ovary. Enzymes showing differences in transcript abundance in mouse and human are the mannosidases, MAN2A1 (Man II) is more abundant in human ovary, while MAN2A1 (Man II) and MAN2A2 (Man IIx) are equally abundant in mouse ovary. Overall, for this subset of genes participating in the *N*-linked pathway, transcript levels in both mouse and human normal ovary show a high degree of species conservation.

3.2 Comparative analysis of normal and epithelial endometrioid ovarian carcinoma

To investigate possible differences in the expression of GT and GH in malignant epithelial ovarian tissue, RNA from mouse endometrioid and human endometrioid carcinoma was analyzed by qRT-PCR. Total RNA from age-matched human normal ovary was purchased from a commercial source. Human normal ovarian tissue samples were averaged for comparison with the qRT-PCR results from individual human tumor tissues. The mouse normal samples qRT-PCR results were also averaged to enable comparison with qRT-PCR results from individual mouse tumor tissues. The levels of MGAT1 and MGAT2 transcripts were increased above normal for both mouse and human tumors suggesting increased complex *N*-linked glycans (Figs. 2A and B). The transcripts encoding FUT8, the enzyme responsible for α(1,6) fucosylation of the core *N*-linked glycan, increased on average 1.5–2-fold relative to normal for mouse tumor tissues (Fig. 2A). However, in human endometrioid ovarian tumors, an increase in FUT8 transcripts occurred in only one of three cases analyzed (Fig. 2B). These results indicate that the factors regulating transcript levels of FUT8 may be more complex in human ovarian cancer. The transcript levels for MGAT3 in both mouse and human tumor samples were increased significantly (average of 18-fold for human and 16-fold for mouse) relative to normal ovarian tissue. The lower transcript abundance of MGAT3 observed for mouse and human normal ovary (Figs. 1B and C) contrast with the large increase in MGAT3 transcripts observed for all cases of epithelial endometrioid carcinoma analyzed in both mouse and human (Figs. 2A and B). The commonality of this change for mouse and human tumor samples along with the magnitude of the change predict the possibility of isolating glycoproteins with complex bisecting *N*-linked glycans as markers for endometrioid ovarian cancer. Transcripts encoding enzymes that perform outer branching of complex *N*-linked glycans such as MGAT4a, MGAT4b, and MGAT5 are increased in mouse and human ovarian cancer relative to normal. MGAT4a transcripts are increased at a higher level relative to normal for mouse compared with human (2–6-fold and 1.5–4-fold, respectively). However, levels of MGAT4b were also elevated in human tumor tissue, while mouse MGAT4b transcript levels in mouse tumor were not significantly increased. The different regulation of MGAT4b transcripts in mouse and human ovarian tumor tissue may highlight a possible species-specific differences in the transcriptional regulation of this gene. However, the cumulative effect of increases in MGAT4a, MGAT4b, and MGAT5 predict more branched complex *N*-linked glycan structures present in endometrioid ovarian cancer relative to normal.

3.3 Comparative lectin analysis

To investigate whether the tumor-specific changes in GT transcript levels correlate with glycan structures found on glycoproteins, we used lectin separation and blotting techniques. The carbohydrate binding preferences for lectins are diverse, allowing the selection of lectins to detect a wide range of oligosaccharide structures. Lectins (E-PHA, L-PHA, DSL, and AAL) recognizing the oligosaccharide products of FUT8, MGAT3, MGAT4a, MGAT4b, MGAT5, and MGAT5b are shown in Fig. 3. These are only examples of oligosaccharide structures that these lectins can bind to and are not intended to be a complete list of all structures capable of binding the lectins. Sugar residues previously described as a determinant for binding of each lectin are circled [17–21]. Con A is a lectin that recognizes branched mannose residues with high affinity (Fig. 3), and this lectin was used to separate the high-mannose, hybrid, and complex biantennary oligosaccharides from the complex tri- and tetra-antennary *N*-linked glycans prior to lectin blot detection [19]. Total cell lysates from the three mouse tumors were pooled for lectin analysis due to the high degree of correspondent changes observed in the qRT-PCR experiments.

3.4 Increased core fucosylation in ovarian tumors

All three mouse endometrioid ovarian tumors analyzed showed elevated levels of FUT8 transcripts (Fig. 2). The lectin AAL has a high affinity for the core α(1,6) fucose linked product that would result from FUT8 activity [17]. Core fucosylation can be found on hybrid type *N*-linked glycans as well as complex bi-, tri-, and tetra-antennary oligosaccharides. However, no differences in AAL binding to Con A bound fractions were observed between normal and tumors, suggesting that the levels of core fucosylation do not change significantly on hybrid type and complex biantennary *N*-linked glycans for ovarian tumors (data not shown). AAL binding to the unbound Con A fraction increases significantly to glycoproteins isolated from ovarian tumors compared to normal ovarian tissue (Fig. 4A lanes 1 and 2). These results indicate that the core fucosylation of complex tri- and tetra-branched oligosaccharides increased for tumors relative to normal. To analyze human ovarian cancer tissues, individual samples were analyzed due to the differences in qRT-PCR results for these cases for FUT8. AAL binding to glycoproteins isolated from human endometrioid ovarian tumors was similar to the levels predicted by qRT-PCR results for case 471. Case 471 had a >4-fold increase in FUT8 mRNA compared with normal and shows seven-fold increase in the level of AAL binding relative to normal (Figs. 2B and 4B, lane 4). Case 711 had similar levels of FUT8 transcripts and shows levels of AAL reactivity similar to the normal control sample (Figs. 2B and 4B, lane 2). Case 741 had lower levels of FUT8 expression compared with normal (Fig. 2B), yet AAL binding was significantly increased (Fig. 4B, lane 3). To better evaluate the fucosylation of this case we used qRT-PCR to analyze all known fucosyltransferases and fucosidases. Our results indicate a two-fold reduction in the levels of α-ʟ-fucosidase (FUCA2) expression (data not shown). We did not observe this decrease in FUTA2 for cases 711 and 471, suggesting that this may be contributing to the increased levels of core α-1,6-fucosylation for case 741. Our data suggest that in the majority of cases for both mouse and human, core fucosylation levels are elevated. Therefore, glycoproteomic studies targeting the core fucose could potentially lead to the isolation of tumor-specific markers for ovarian cancer.

3.5 Ovarian tumors have increased levels of bisecting complex *N*-linked glycans

N-glycans containing a bisecting *N*-acetylglucosamine are produced by the activity of MGAT3 (Fig. 1A). This enzyme showed the largest increases in expression in ovarian tumor tissues compared with normal ovary tissue (Figs. 2A and B). Lectin analysis of mouse tissues using the lectin E-PHA, whose binding is dependent on the presence of bisecting GlcNAc (Fig. 3), shows >2× the levels of E-PHA binding for tumor relative to normal (Fig.

4A, lanes 3 and 4). Human ovarian tumor glycoproteins analyzed for E-PHA binding showed positive correlation with qRT-PCR results for each case. For example, case 471 and 741 had the highest and second highest increases in MGAT3 transcript levels (Fig. 2B) and these cases also have the highest levels of E-PHA binding (Fig. 4B, lanes 7 and 8). Case 711 had a lower increase in MGAT3 transcripts measured by qRT-PCR and shows a lower level of E-PHA binding than cases 471 and 741. In every endometrioid ovarian tumor analyzed, mouse and human, there were elevated bisecting complex *N*-linked glycans compared with normal controls. Although the datasets are small, these results strongly suggest that the presence of bisecting complex *N*-glycans is a marker for ovarian tumors.

3.6 Tri- or tetra-antennary complex *N*-linked glycans are increased in ovarian tumors

The lectins known as DSL and L-PHA recognize the outer branches of complex *N*-linked glycans (MGAT4a, MGAT4b, MGAT5, and MGAT5b) (Fig. 3). L-PHA is specific for the β(1,6) branched, galactosylated product of MGAT5; while DSL can recognize the β(1,4) branch added by MGAT4a and MGAT4b as well as the MGAT5 branch (Fig. 3). MGAT4a and MGAT4b transcript levels were elevated for human endometrioid ovarian tumors and MGAT4a transcripts were amplified for mouse tumors (Figs. 2A and B). These genes can perform the same glycosyltransferase reactions and their elevations predict the existence of more β(1,4) branched glycans and increased DSL binding. Indeed, analysis of unbound Con A fractions indicate elevated levels of DSL binding to mouse tumor glycoproteins compared with glycoproteins from normal mouse ovary (Fig. 4A, lanes 5 and 6). The levels of DSL binding to tumor glycoproteins isolated from human ovarian tumors were lower compared with AAL or E-PHA binding (Fig. 4B, lanes 9–12) and this correlates with a lower change in transcript levels for MGAT4 (Fig. 2B). Interestingly, L-PHA binding levels for mouse ovarian tumor tissues were not increased above normal, despite increases in MGAT5 transcripts (Figs. 2A and 4A, lanes 7 and 8). Human tumor samples had higher levels of MGAT5 transcripts compared with normal and do show a slight increase in L-PHA binding compared with normal (Figs. 2B and 4B, lanes 13–16). Mouse ovarian tumors had a two-fold increase in MGAT5 and human ovarian tumors had a three- to five-fold increase in MGAT5 expression (Figs. 2A and B and Table 1). Based on these findings elevated L-PHA binding would be expected. However, we find no increase in L-PHA binding for mouse ovarian tumors (Fig. 4A) and a lower than expected increase in L-PHA reactivity to glycoproteins from human ovarian tumors. These results may indicate that the MGAT3 elevated activity may inhibit MGAT5 activity and this will be discussed further in the discussion. Overall, the DSL lectin is useful for capturing glycoproteins with the MGAT4 or MGAT5 branch, and based on our analysis, would be an effective lectin for isolating glycoprotein markers with elevated β(1,4) or β(1,6) complex branched glycans for endometrioid ovarian tumors.

4 Discussion

In this report we have used a glycotranscriptome approach to characterize the *N*-linked glycan profiles of normal ovary and endometrioid ovarian carcinoma. Our results provide several significant findings: (i) mouse and human normal ovarian tissues have a similar expression profile for certain enzymes participating in the formation of *N*-linked glycans suggesting some degree of species conservation, (ii) enzymes changing in expression for tumors isolated from the mouse model of human endometrioid ovarian cancer correspond qualitatively with changes observed for human tumors of the same malignancy, (iii) E-PHA, AAL, and DSL reactivity levels were elevated in endometrioid ovarian tumors relative to normal indicating that these lectins could be useful together for biomarker discovery or to improve the specificity of existing ovarian tumor markers.

4.1 Glycosylation changes observed for reproductive malignancies

Analysis of glycoprotein glycosylation patterns is emerging as a powerful tool to discriminate normal glycoproteins from glycoproteins marking diseases such as cancer. Over 20 years ago, researchers began to observe glycosylation changes occurring on cell surface glycoproteins following oncogenic transformation [1, 2, 22, 23]. For breast cancer, increased β(1,6) branched glycans emerged qualitatively from the transition to malignancy due to elevated expression of the MGAT5 gene [24, 25]. Few studies have evaluated glycosylation changes for ovarian cancer [26–29], however, from the small group of studies conducted, Rudd and coworkers [27] found increased levels of bisecting core fucosylated complex *N*-linked glycans in the serum of ovarian cancer patients compared with normal serum. This result agrees with our data showing increased core fucosylation and bisecting glycans in endometrioid ovarian tumor tissues. Therefore, there is a high probability of isolating and identifying glycoproteins shed into serum from ovarian carcinomas with differences in glycosylation. Lebrilla [26] have monitored changes in glycan structures in the serum of ovarian cancer patients using MALDI-FTMS and find several tumor-specific changes for neutral oligosaccharides in MALDI spectra. This study employed a β-elimination procedure to remove oligosaccharides, therefore the neutral glycans changing in the serum could correspond to *N*- or *O*-linked glycans. Our data suggest that neutral glycans from the *N*-linked biosynthetic pathway such as core fucosylation and bisecting *N*-acetylglucosamine are increased significantly in ovarian tumor tissue relative to normal. Therefore, it should be possible to identify the glycoproteins that have these neutral *N*-linked glycan alterations from patient serum. In conclusion, our data in addition to these previous studies indicate that like breast cancer, ovarian tumor formation results in distinct altered glycan structures.

4.2 Comparison of changes in glycosylation between a mouse-model of endometrioid ovarian cancer and human endometrioid ovarian cancer

Ovarian tumors derived from the mouse model of human endometrioid ovarian cancer developed by Dinulescu *et al*. [12] are well differentiated and recapitulate human ovarian cancer histologically. The benefits of mouse models are numerous, including: stable genetics, controlled environmental factors such as diet, and most importantly, the ability to sample tissue and serum at different stages of tumor development. Our data demonstrate that the glycomic changes occurring in the *N*-linked pathway for mouse-derived epithelial endometrioid ovarian tumors show corresponding changes in human ovarian endometrioid tumors.

4.3 Increased knowledge about the *N*-linked glycan pathway

The *N*-linked glycosylation pathway consists of a series of sequential reactions (Fig. 1A). The qRT-PCR approach enabled the quantization of the transcript levels for several enzymes with a wide dynamic range. The total pathway approach offers a chance to learn more about how synchronous oncogenic signaling changes can influence glycosylation. A summary of the average fold changes in expression measured for each enzyme analyzed is provided in Table 1. Some interesting findings that have resulted from this study include: (i) increased variability in FUT8 levels for human ovarian cancer versus mouse tumors, suggesting more complex influences controlling the levels of core fucosylation, (ii) lower levels of L-PHA reactivity for glycoproteins with elevated MGAT5 mRNA levels suggests possible inhibition of MGAT5 activity by MGAT3.

Genetic factors influencing glycosylation patterns have not been extensively studied. Although there has been a study recently published examining the effect of single-nucleotide polymorphisms in genes involved in the mucin-type glycosylation of MUC1 [30]. This study found that genetic polymorphisms within glycosylation enzymes analyzed for MUC1 may

be playing a role in the under-glycosylation of this protein in ovarian cancer patients suggesting that genetic factors can effect glycosylation. Several of the GT and GH enzymes included in this study are located in similar regions of the chromosomes (Table 1). MGAT1 and MGAT4b are located on the same chromosome in close proximity and show very different expression profiles for ovarian cancer. This seems to suggest that elevations in MGAT1 expression are probably not related to gain of chromosome copy, or MGAT4b would be increased in a similar manner. The changes in expression observed for GT enzymes in ovarian cancer could be due to differences in factors regulating GT promoters.

The small sample size of human endometrioid carcinoma cases analyzed in our study suggests that FUT8 expression and activity are more variable. Due to the lack of variability in the mouse model, we postulate that in humans there may be unknown factors in ovarian tumors either genetic or epigenetic that are capable of influencing core fucosylation. The FUT8 variability in human ovarian tumors contrasts with MGAT1, MGAT2, and MGAT3 which seems to be unaffected by genetic differences. More studies examining the glycomic changes in human cancer samples performed in conjunction with murine models are needed to better understand the possible role of genetic regulation on glycosylation.

The products of MGAT3 activity, the bisecting *N*-acetylglucosamine structure, has been reported to inhibit the activity of MGAT5 [31, 32]. We find that MGAT3 levels are substantially increased far above MGAT5 levels in ovarian tumors. Therefore, one possibility for why we observe less change in L-PHA reactivity for ovarian tumors (Figs. 4A and B), despite increased levels of MGAT5 expression, may be that the addition of bisecting *N*-acetylglucosamine by MGAT3 prevented the addition of the β(1,6) branched oligosaccharide structure. Competition for the same nucleotide sugar donor (UDP-GlcNAc) does not seem to be a factor since MGAT4a and MGAT4b addition (evidenced by DSL binding) is unaffected by the large increase in MGAT3 activity. The addition of bisecting *N*-acetylglucosamine to the trimannosyl core *N*-linked glycan has been reported to occur in opposition to β(1,6) branching performed by MGAT5 during the cell cycle [33]. In this study the authors found that the mRNA levels and protein levels for MGAT5 were not changing, yet there was less MGAT5 enzyme activity at stages of the cell cycle when MGAT3 activity levels were high. These data along with our data support the notion that increased MGAT3 activity inhibits the addition of β(1,6) branched glycans by MGAT5 and the mechanism of this inhibition is currently unknown.

4.4 Bisecting oligosaccharides and cancer

Elevated levels of MGAT3 expression and an increase in bisecting glycans have been reported for pancreatic cancer and hepatoma [34, 35]. Studies using diethylnitrosamine to induce liver tumor formation in mice null for MGAT3 showed reduced tumor formation [29, 36]. However, if MGAT3 was overexpressed there is no induction or augmentation of tumor growth using diethylnitrosamine [37]. This result suggests an indirect effect of MGAT3 overexpression on liver tumorigenesis. In ovarian tumors, bisecting glycan structures predominate as evidenced by increased MGAT3 mRNA (Figs. 2A and B) and elevated E-PHA binding (Figs. 4A and B). Bisecting structures have also been documented on CA125 isolated from the ovarian cancer cell line OVCAR3 [28]. Mice null for MGAT3 are viable and reproduce normally. This, along with the fact that MGAT3 is expressed at a low level in normal ovary, suggest that therapeutic strategies targeting MGAT3 could be useful for retarding ovarian tumor progression with minimal interruption of normal ovary functions.

In conclusion, the glycomic analysis presented in this manuscript provides a framework for future glycoproteomic studies. These studies will enable the identification of the proteins that express bisecting *N*-linked glycans and allow for the structural characterization of the bisecting oligosaccharides.

Supplementary Material

Refer to Web version on PubMed Central for supplementary material.

Acknowledgments

K. L. A. is supported by a fellowship from the American Cancer Society and the Canary Fund. D. M. D. is supported by the Burroughs-Wellcome Foundation, the Harvard Ovarian Cancer Spore Award, the Madeline Franchi Investigator Award, Canary Fund, Mouse Models of Human Cancer Consortium (NCI), and the Ovarian Cancer Research Fund. This work was supported in part by the Burroughs Welcome Foundation (D. M. D.), Rivkin Foundation (D. M. D.), Canary Foundation (D. M. D.), Mary Franchi Award (D. M. D.), the Mouse Models of Human Cancer Consortium (D. M. D.), and the NCRR Center for Biomedical Glycomics P41RR018502, UO/CA128454 and R01CA064462 (M. P.).

Abbreviations

GH	glycosylhydrolases
GT	glycosyltransferases
qRT-PCR	quantitative real-time PCR

References

1. Pierce M, Arango J. Rous sarcoma virus-transformed baby hamster kidney cells express higher levels of asparagine-linked tri- and tetraantennary glycopeptides containing [GlcNAc-beta (1,6)Man-alpha (1,6)Man] and poly-*N*-acetyllactosamine sequences than baby hamster kidney cells. J. Biol. Chem. 1986; 261:10772–10777. [PubMed: 3015940]
2. Meezan E, Wu HC, Black PH, Robbins PW. Comparative studies on the carbohydrate-containing membrane components of normal and virus-transformed mouse fibroblasts. II. Separation of glycoproteins and glycopeptides by sephadex chromatography. Biochemistry. 1969; 8:2518–2524. [PubMed: 4307997]
3. Guo HB, Lee I, Kamar M, Akiyama SK, Pierce M. Aberrant *N*-glycosylation of beta1 integrin causes reduced alpha5beta1 integrin clustering and stimulates cell migration. Cancer Res. 2002; 62:6837–6845. [PubMed: 12460896]
4. Guo HB, Lee I, Kamar M, Pierce M. *N*-acetylglucosaminyltransferase V expression levels regulate cad-herin-associated homotypic cell–cell adhesion and intracellular signaling pathways. J. Biol. Chem. 2003; 278:52412–52424. [PubMed: 14561752]
5. Guo HB, Randolph M, Pierce M. Inhibition of a specific *N*-glycosylation activity results in attenuation of breast carcinoma cell invasiveness-related phenotypes: inhibition of epidermal growth factor-induced dephosphorylation of focal adhesion kinase. J. Biol. Chem. 2007; 282:22150–22162. [PubMed: 17537730]
6. Abbott KL, Troupe K, Lee I, Pierce M. Integrin-dependent neuroblastoma cell adhesion and migration on laminin is regulated by expression levels of two enzymes in the *O*-mannosyl-linked glycosylation pathway, PomGnT1 and GnT-Vb. Exp. Cell Res. 2006; 312:2837–2850. [PubMed: 16857188]
7. Nairn AV, Kinoshita-Toyoda A, Toyoda H, Xie J, et al. Glycomics of proteoglycan biosynthesis in murine embryonic stem cell differentiation. J. Proteome Res. 2007; 6:4374–4387. [PubMed: 17915907]
8. Ozols RF, Bookman MA, Connolly DC, Daly MB, et al. Focus on epithelial ovarian cancer. Cancer Cell. 2004; 5:19–24. [PubMed: 14749123]
9. Hayat MJ, Howlader N, Reichman ME, Edwards BK. Cancer statistics, trends, and multiple primary cancer analyses from the surveillance, epidemiology, and end results (SEER) Program. Oncologist. 2007; 12:20–37. [PubMed: 17227898]

10. Orsulic S, Li Y, Soslow RA, Vitale-Cross LA, et al. Induction of ovarian cancer by defined multiple genetic changes in a mouse model system. Cancer Cell. 2002; 1:53–62. [PubMed: 12086888]
11. Aunoble B, Sanches R, Didier E, Bignon YJ. Major oncogenes and tumor suppressor genes involved in epithelial ovarian cancer (review). Int. J. Oncol. 2000; 16:567–576. [PubMed: 10675491]
12. Dinulescu DM, Ince TA, Quade BJ, Shafer SA, et al. Role of K-ras and Pten in the development of mouse models of endometriosis and endometrioid ovarian cancer. Nat. Med. 2005; 11:63–70. [PubMed: 15619626]
13. Lee Y, Miron A, Drapkin R, Nucci MR, et al. candidate precursor to serous carcinoma that originates in the distal fallopian tube. J. Pathol. 2007; 211:26–35. [PubMed: 17117391]
14. Auersperg N, Wong AS, Choi KC, Kang SK, Leung PC. Ovarian surface epithelium: Biology, endocrinology, and pathology. Endocr. Rev. 2001; 22:255–288. [PubMed: 11294827]
15. Irving JA, Catasus L, Gallardo A, Bussaglia E, et al. Synchronous endometrioid carcinomas of the uterine corpus and ovary: Alterations in the beta-catenin (CTNNB1) pathway are associated with independent primary tumors and favorable prognosis. Hum. Pathol. 2005; 36:605–619. [PubMed: 16021566]
16. Kolasa IK, Rembiszewska A, Janiec-Jankowska A, Dansonka-Mieszkowska A, et al. PTEN mutation, expression and LOH at its locus in ovarian carcinomas. Relation to TP53, K-RAS and BRCA1 mutations. Gynecol. Oncol. 2006; 103:692–697. [PubMed: 16793127]
17. Nagata Y, Fukumori F, Sakai H, Hagiwara T, et al. Crystallization and characterization of a lectin obtained from a mushroom *Aleuria aurantia*. Biochim. Biophys. Acta. 1991; 1076:187–190. [PubMed: 1998719]
18. Wimmerova M, Mitchell E, Sanchez JF, Gautier C, Imberty A. Crystal structure of fungal lectin: Six-bladed beta-propeller fold and novel fucose recognition mode for *Aleuria aurantia* lectin. J. Biol. Chem. 2003; 278:27059–27067. [PubMed: 12732625]
19. Cummings RD, Kornfeld S. Fractionation of asparagine-linked oligosaccharides by serial lectin-agarose affinity chromatography. A rapid, sensitive, and specific technique. J. Biol. Chem. 1982; 257:11235–11240. [PubMed: 7118881]
20. Cummings RD, Kornfeld S. Characterization of the structural determinants required for the high affinity interaction of asparagine-linked oligosaccharides with immobilized *Phaseolus vulgaris* leukoagglutinating and erythroagglutinating lectins. J. Biol. Chem. 1982; 257:11230–11234. [PubMed: 7118880]
21. Yamashita K, Totani K, Ohkura T, Takasaki S, et al. Carbohydrate binding properties of complex-type oligosaccharides on immobilized *Datura stramonium* lectin. J. Biol. Chem. 1987; 262:1602–1607. [PubMed: 3805046]
22. Kobata A, Amano J. Altered glycosylation of proteins produced by malignant cells, and application for the diagnosis and immunotherapy of tumours. Immunol. Cell Biol. 2005; 83:429–439. [PubMed: 16033539]
23. Hakomori S. Antigen structure and genetic basis of histoblood groups A, B and O: Their changes associated with human cancer. Biochim. Biophys. Acta. 1999; 1473:247–266. [PubMed: 10580143]
24. Buckhaults P, Chen L, Fregien N, Pierce M. Transcriptional regulation of *N*-acetylglucosaminyltransferase V by the src oncogene. J. Biol. Chem. 1997; 272:19575–19581. [PubMed: 9235963]
25. Fernandes B, Sagman U, Auger M, Demetrio M, Dennis JW. Beta 1–6 branched oligosaccharides as a marker of tumor progression in human breast and colon neoplasia. Cancer Res. 1991; 51:718–723. [PubMed: 1985789]
26. An HJ, Miyamoto S, Lancaster KS, Kirmiz C, et al. Profiling of glycans in serum for the discovery of potential biomarkers for ovarian cancer. J. Proteome Res. 2006; 5:1626–1635. [PubMed: 16823970]
27. Saldova R, Royle L, Radcliffe CM, Abd Hamid UM, et al. Ovarian cancer is associated with changes in glycosylation in both acute-phase proteins and IgG. Glycobiology. 2007; 17:1344–1356. [PubMed: 17884841]

28. Kui Wong N, Easton RL, Panico M, Sutton-Smith M, et al. Characterization of the oligosaccharides associated with the human ovarian tumor marker CA125. J. Biol. Chem. 2003; 278:28619–28634. [PubMed: 12734200]
29. Wang PH, Lee WL, Juang CM, Yang YH, et al. Altered mRNA expressions of sialyltransferases in ovarian cancers. Gynecol. Oncol. 2005; 99:631–639. [PubMed: 16112178]
30. Sellers TA, Huang Y, Cunningham J, Goode EL, et al. Association of single nucleotide polymorphisms in glycosylation genes with risk of epithelial ovarian cancer. Cancer Epidemiol. Biomarkers Prev. 2008; 17:397–404. [PubMed: 18268124]
31. Yoshimura M, Nishikawa A, Ihara Y, Taniguchi S, Taniguchi N. Suppression of lung metastasis of B16 mouse melanoma by *N*-acetylglucosaminyltransferase III gene transfection. Proc. Natl. Acad. Sci. USA. 1995; 92:8754–8758. [PubMed: 7568011]
32. Taniguchi N, Yoshimura M, Miyoshi E, Ihara Y, et al. Remodeling of cell surface glycoproteins by *N*-acetylglucosaminyltransferase III gene transfection: Modulation of metastatic potentials and down regulation of hepatitis B virus replication. Glycobiology. 1996; 6:691–694. [PubMed: 8953279]
33. Guo HB, Jiang AL, Ju TZ, Chen HL. Opposing changes in *N*-acetylglucosaminyltransferase-V and -III during the cell cycle and all-trans retinoic acid treatment of hepatocarcinoma cell line. Biochim. Biophys. Acta. 2000; 1495:297–307. [PubMed: 10699467]
34. Ishibashi K, Nishikawa A, Hayashi N, Kasahara A, et al. *N*-acetylglucosaminyltransferase III in human serum, and liver and hepatoma tissues: Increased activity in liver cirrhosis and hepatoma patients. Clin. Chim. Acta. 1989; 185:325–332. [PubMed: 2482796]
35. Nan BC, Shao DM, Chen HL, Huang Y, et al. Alteration of *N*-acetylglucosaminyltransferases in pancreatic carcinoma. Glycoconj. J. 1998; 15:1033–1037. [PubMed: 10211708]
36. Bhaumik M, Harris T, Sundaram S, Johnson L, et al. Progression of hepatic neoplasms is severely retarded in mice lacking the bisecting *N*-acetylglucosamine on *N*-glycans: Evidence for a glycoprotein factor that facilitates hepatic tumor progression. Cancer Res. 1998; 58:2881–2887. [PubMed: 9661906]
37. Stanley P. Biological consequences of overexpressing or eliminating *N*-acetylglucosaminyltransferase-TIII in the mouse. Biochim. Biophys. Acta. 2002; 1573:363–368. [PubMed: 12417419]
38. Nairn AV, York WS, Harris K, Hall EM, et al. Regulation of glycan structures in animal tissues: Transcript profiling of glycan-related genes. J. Biol. Chem. 2008; 283:17298–17313. [PubMed: 18411279]

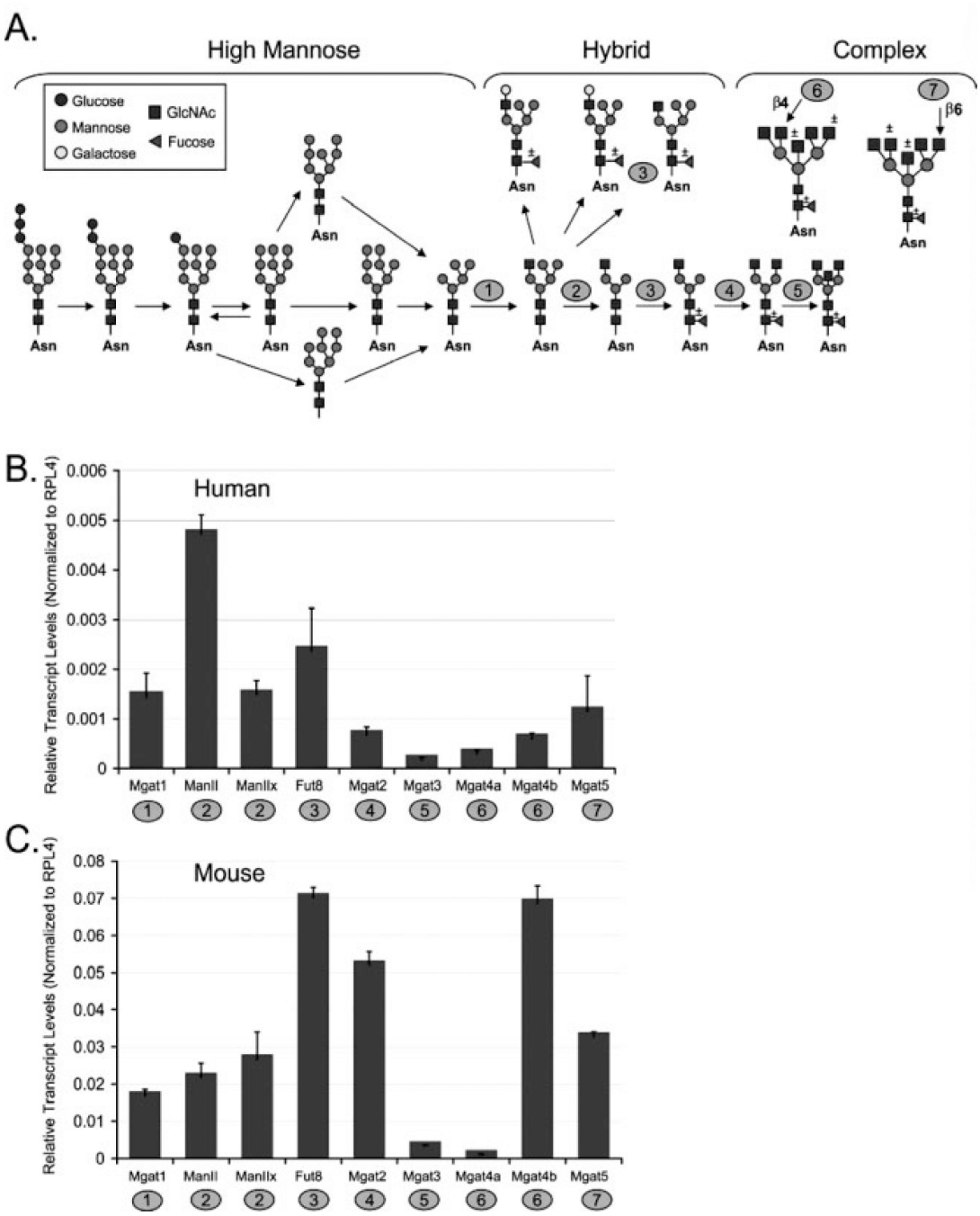

Figure 1.

Transcript analysis of enzymes acting in the *N*-linked pathway for normal ovary. (A) *N*-linked glycosylation pathway with enzymes included in analysis numbered as follows: 1, MGAT1; 2, MAN2A1 (Man II) or MAN2A2 (Man IIx); 3, FUT8; 4, MGAT2; 5, MGAT3; 6, MGAT4a or MGAT4b; 7, MGAT5. (B) Relative transcript levels for normal human ovary tissue, average Ct for two pooled cases. Error bars represent the SD from the mean for triplicate Ct values. (C) Relative transcript levels for normal mouse ovary, average Ct for six pooled normal ovaries. Error bars represent the SD from the mean for triplicate Ct values.

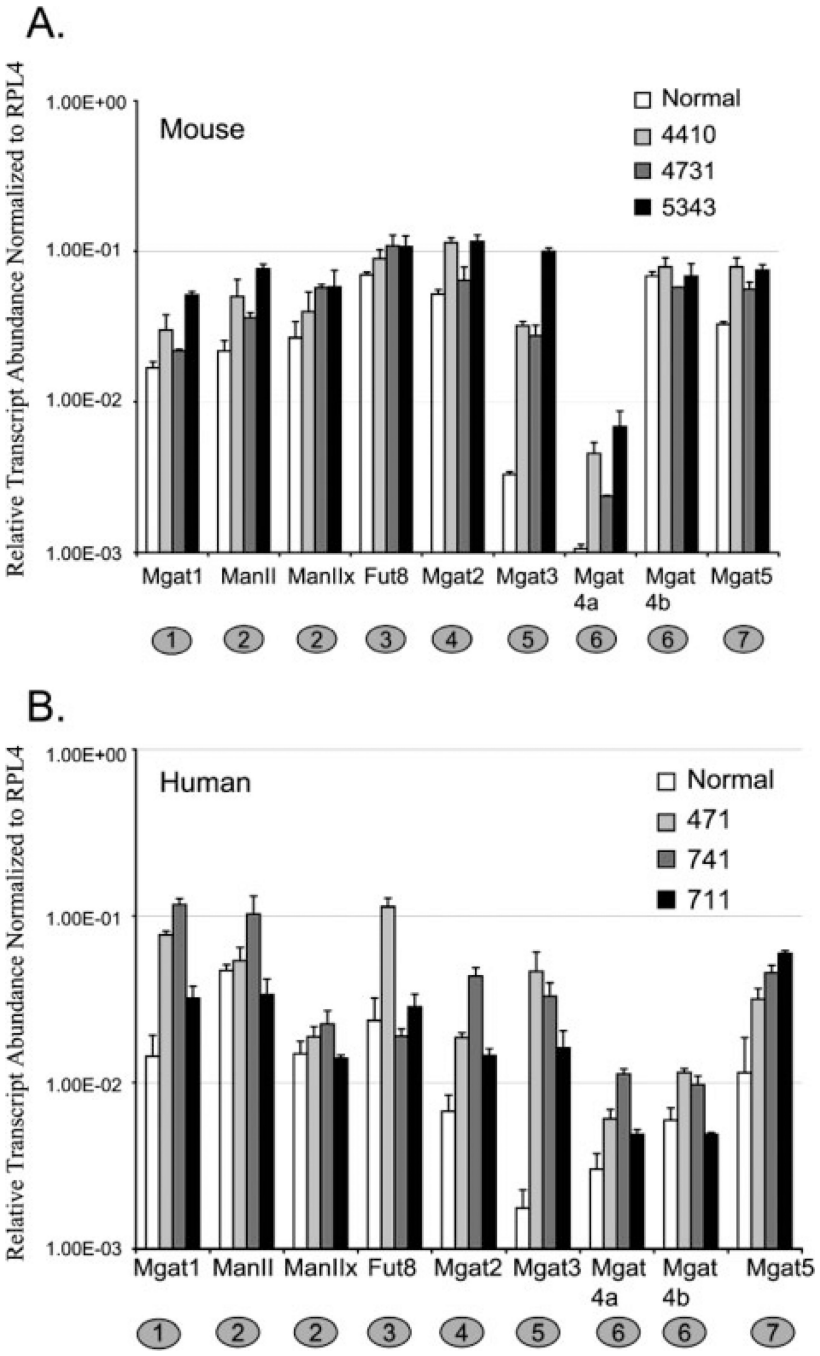

Figure 2.

Comparative analysis of normal and endometrioid ovarian carcinoma. (A) Relative transcript abundance for mouse normal and ovarian tumors plotted on a log scale. Error bars represent the SD from the mean for triplicate Ct values. (B) Relative transcript abundance for human normal and ovarian tumors plotted on a log scale. Error bars represent the SD from the mean for triplicate Ct values.

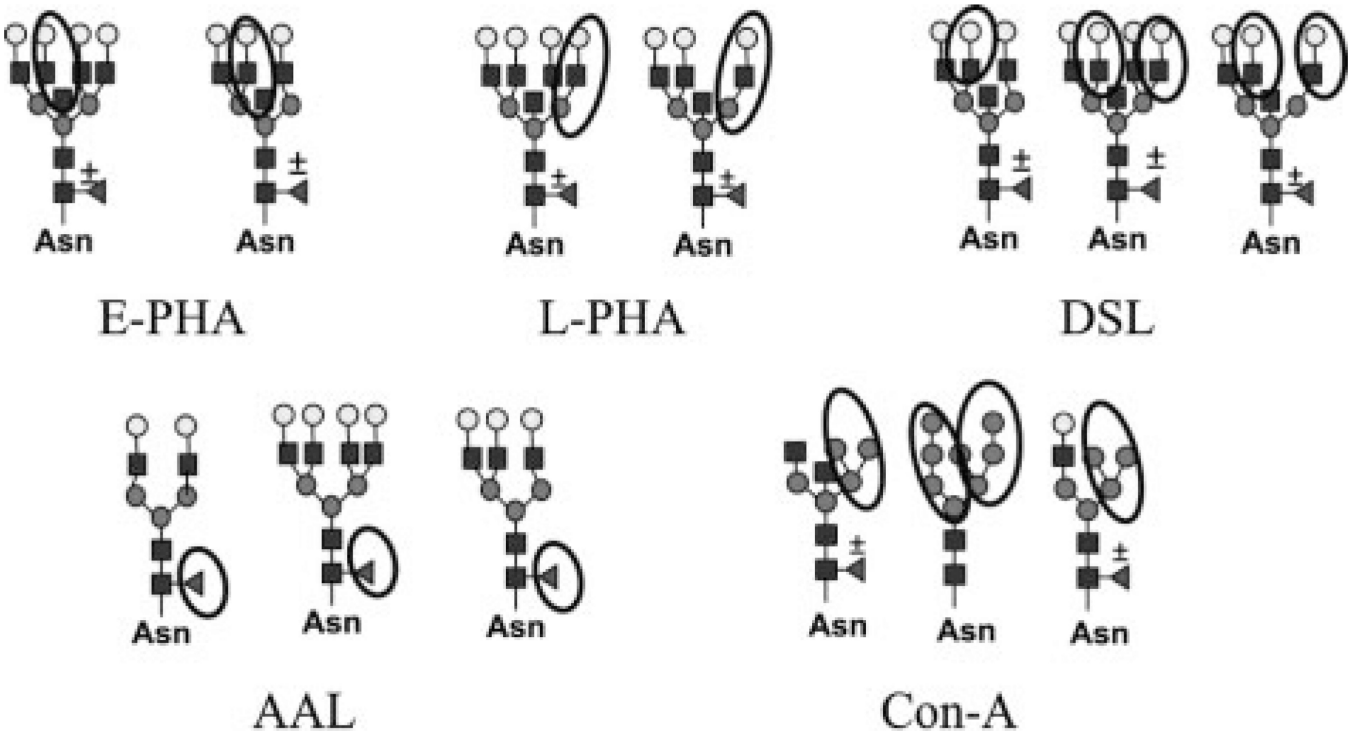

Figure 3.
Oligosaccharides determinants for lectin binding affinity. Examples of structures with important binding determinants from each lectin circled.

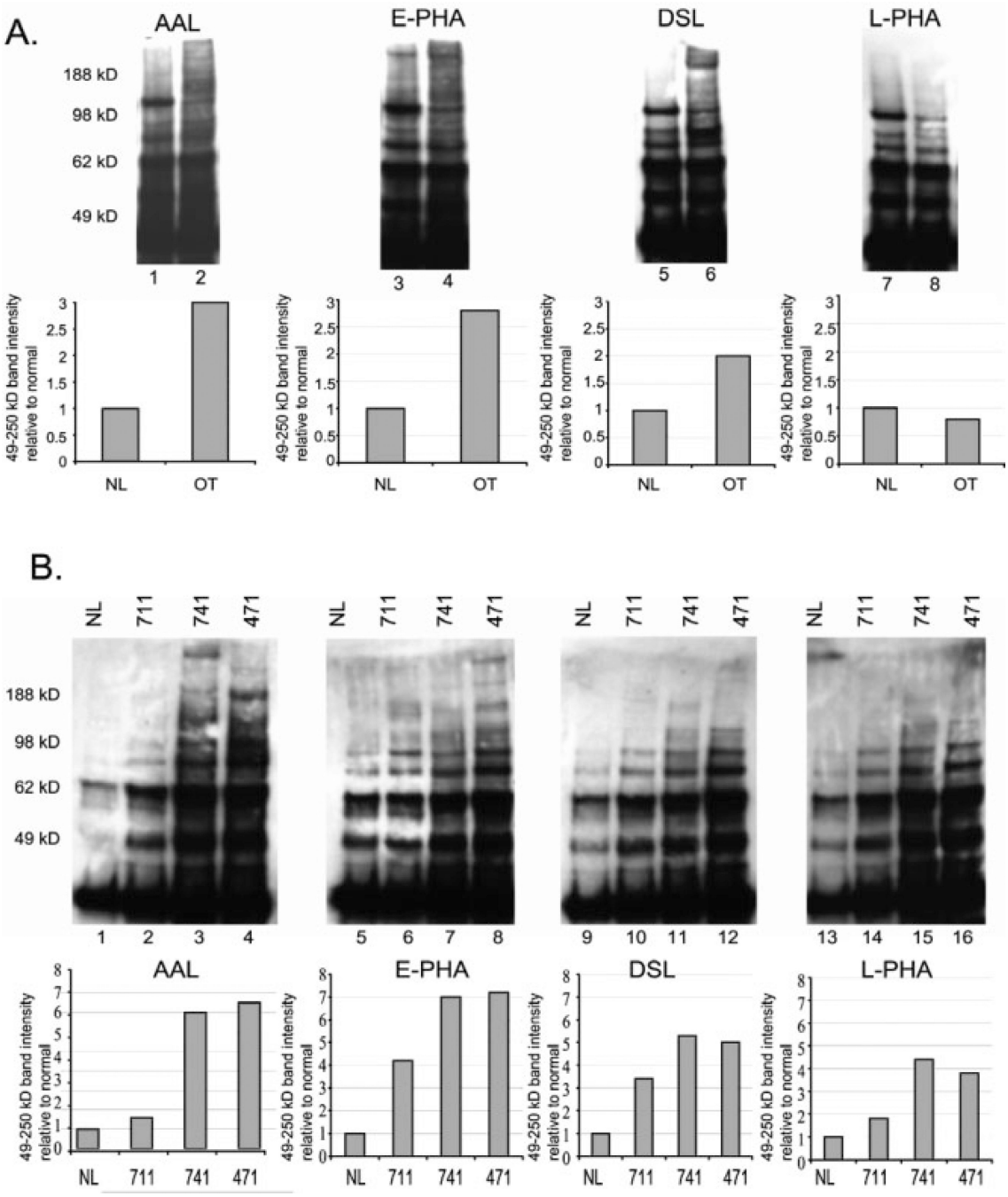

Figure 4.

Lectin blot analysis of glycoproteins from mouse and human endometrioid ovarian carcinoma. (A) Glycoproteins extracted from mouse endometrioid ovarian tumors (lanes 2, 4, 6, and 8) or normal mouse ovary (lanes 1, 3, 5, and 7) that were nonadherent to Con A were separated on 4–12% Bis-Tris gels before transfer to PVDF membrane and detection using biotinylated lectins and streptavidin–HRP. Panel below shows the densitometry analysis of bands from normal (NL) or ovarian tumor (OT) in the 49–250 kDa range from the blots shown above with normal set at 1.0 for comparison. Fold increase was adjusted for lectin pull-down inputs based on the levels of ERK2 on a 10% input blot (data not shown). (B) Glycoproteins nonadherent to Con A from human endometrioid ovarian cancer cases

(711, 741, and 471) and normal human ovary (NL) were separated on 4–12% Bis-Tris gels before lectin blot detection as described. The panel below represents the densitometry results for glycoproteins 49–250 kDa relative to normal set at 1.0. Increases relative to normal were adjusted for input using ERK2 analysis form 10% input blots (data not shown).

Table 1

Genes analysed by qRT-PCR

Symbol	Average fold change mouse	Average fold change human	Chromosome location	Mouse	Human
Fut8	(+) 1.5	(+) 2.3	14q24.3	NM_016893	NM_178154
Mgat1	(+) 2.0	(+) 5.2	5q31 or 5q35	NM_010794	NM_002406
Mgat2	(+) 1.9	(+) 3.8	14q21	NM_146035	NM_002408
Mgat3	(+) 16.0	(+) 18.2	22q13.1	NM_010795	NM_002409
Mgat4a	(+) 4.4	(+) 2.5	2q12	NM_173870	NM_012214
Mgat4b	No change	(+) 1.5	5q35	NM_145926	NM_014275/NM_054013
Mgat5	(+) 2.2	(+) 4.0	2q21	NM_145128	NM_002410
MAN2A1	(+) 2.5	(+) 1.4	5q21	NM_008549	NM_002372
MAN2A2	(+) 1.9	(+) 1.2	15q25	NM_172903	NM_006122